An interferometric current sensor based on optical fiber micro wires

Mohammad Belal,[1] Zhang-qi Song,[1,2] Yongming Jung,[1] Gilberto Brambilla,[1] and Trevor Newson[1]

[1]*Optoelectronics Research Centre, University of Southampton, Southampton, SO17 1BJ, UK*
[2]*College of Optoelectronic Science and Engineering, National University of Defense Technology, Changsha 410073, China*
songzhangqi@nudt.edu.cn

Abstract: In this paper we demonstrate a compact current sensor using the optic fiber micro wire, based on the idea of interferometrically measuring the thermally induced optical phase shifts as a result of heat produced due to the flow of electric current over short transit lengths. A responsivity of 1.28×10^{-4} rad/I^2 at 50Hz of current signal has been shown, with capability of measuring alternating current signals up to 500Hz.

OCIS codes: (060.2370) Fiber optics sensors; (060.2310) Fiber optics;

References and links

1. G. Brambilla, "Optical fibre nanowires and microwires: a review," J. Opt. **12**(4), 043001 (2010).
2. L. Tong, "Brief introduction to optical microfibers and nanofibers," Front. Optoelectron. China **3**(1), 54–60 (2010).
3. J. Lou, L. Tong, and Z. Ye, "Modeling of silica nanowires for optical sensing," Opt. Express **13**(6), 2135–2140 (2005).
4. J. Villatoro, and D. Monzón-Hernández, "Fast detection of hydrogen with nano fiber tapers coated with ultra thin palladium layers," Opt. Express **13**(13), 5087–5092 (2005).
5. L. Zhang, F. Gu, J. Lou, X. Yin, and L. Tong, "Fast detection of humidity with a subwavelength-diameter fiber taper coated with gelatin film," Opt. Express **16**(17), 13349–13353 (2008).
6. F. Gu, L. Zhang, X. Yin, and L. Tong, "Polymer single-nanowire optical sensors," Nano Lett. **8**(9), 2757–2761 (2008).
7. F. Xu, P. Horak, and G. Brambilla, "Optical microfiber coil resonator refractometric sensor," Opt. Express **15**(12), 7888–7893 (2007).
8. F. Xu, and G. Brambilla, "Demonstration of a refractometric sensor based on optical microfiber coil resonator," Appl. Phys. Lett. **92**(10), 101126 (2008).
9. P. Polynkin, A. Polynkin, N. Peyghambarian, and M. Mansuripur, "Evanescent field-based optical fiber sensing device for measuring the refractive index of liquids in microfluidic channels," Opt. Lett. **30**(11), 1273–1275 (2005).
10. C.-Y. Chao, and L. Jay Guo, "Design and Optimization of Microring Resonators in Biochemical Sensing Applications," J. Lightwave Technol. **24**(3), 1395–1402 (2006).
11. N. Vukovic, N. G. R. Broderick, M. N. Petrovich, and G. Brambilla, "Novel method for the fabrication of long optical tapers," IEEE Photon. Technol. Lett. **20**(14), 1264–1266 (2008).
12. L. M. Tong, R. R. Gattass, J. B. Ashcom, S. L. He, J. Y. Lou, M. Y. Shen, I. Maxwell, and E. Mazur, "Subwavelength-diameter silica wires for low-loss optical wave guiding," Nature **426**(6968), 816–819 (2003).
13. G. Brambilla, V. Finazzi, and D. J. Richardson, "Ultra-low-loss optical fiber nanotapers," Opt. Express **12**(10), 2258–2263 (2004).
14. F. Xu, and G. Brambilla, "Embedding optical microfiber coil resonators in Teflon," Opt. Lett. **32**(15), 2164–2166 (2007).
15. F. Xu, and G. Brambilla, "Preservation of Micro-Optical Fibers by Embedding," Jpn. J. Appl. Phys. **47**(8), 6675–6677 (2008).
16. N. Lou, R. Jha, J. L. Domínguez-Juárez, V. Finazzi, J. Villatoro, G. Badenes, and V. Pruneri, "Embedded optical micro/nano-fibers for stable devices," Opt. Lett. **35**(4), 571–573 (2010).
17. Y. Jung, S. R. Han, S. Kim, U. C. Paek, and K. Oh, "Versatile control of geometric birefringence in elliptical hollow optical fiber," Opt. Lett. **31**(18), 2681–2683 (2006).
18. Y. Jung, G. Brambilla, K. Oh, and D. J. Richardson, "Highly birefringent silica microfiber," Opt. Lett. **35**(3), 378–380 (2010).
19. B. Lee, "Review of the present status of optical fiber sensors," Opt. Fiber Technol. **9**(2), 57–79 (2003).
20. R. I. Laming, and D. N. Payne, "Electric Current Sensors Employing Spun Highly Birefringent Optical Fibers," J. Lightwave Technol. **7**(12), 2084–2094 (1989).

#130605 - $15.00 USD Received 24 Jun 2010; revised 30 Aug 2010; accepted 30 Aug 2010; published 3 Sep 2010

21. A. Dandridge, A. B. Tveten, and T. G. Giallorenzi, "Interferometric current sensors using optical fibres," Electron. Lett. **17**(15), 523–525 (1981).
22. W.-W. Lin, "Fiber-optic current sensor," Opt. Eng. **42**(4), 896–897 (2003).
23. G. L. Tangonan, D. I. Persechini, R. J. Morrison, and J. A. Wysocki, "Current sensing with metal coated multimode optic fibers," Electron. Lett. **16**(25-26), 958–959 (1980).
24. K. Böhm, and K. Petermann, "Signal processing schemes for the fiber-optic gyroscope," Proc. SPIE **719**, 36–44 (1986).
25. D. A. Jackson, "Recent progress in monomode fibre-optic sensors," Meas. Sci. Technol. **5**(6), 621–638 (1994).

1. Introduction

In recent years, optical fiber nano wires and micro wires (OFNM) have received considerable attention due to a number of interesting optical properties such as large evanescent field, strong confinement, configurability and robustness [1,2]. One of the attractions of OFNM's is their flexibility compared to that of normal optical fibers. OFNM offers bend radii of the order of a few microns, allowing for packaging of more complex and compact devices. High sensitivities to environment [3] due to large evanescent fields, have lead to utilization of OFNM's as hydrogen, humidity, refractometric and biochemical sensors [4–10] as well. These sensors present excellent properties such as high sensitivity and fast response. In recent years there have been several important advances in OFNM that have contributed towards their increased use for optical sensing, such as recent fabrication techniques of low-loss fiber tapers allow OFNM with lengths from a few millimeters to tens of meters [11–13], thereby increasing their interaction length, embedding/packaging techniques with low refractive index materials have solved problems of device stability [14–16] and the preservation of polarization state with usage of rectangular shaped OFNM with high birefringence [17,18]. All these advances make the OFNM a perfect contender for next generation optical sensing.

Current sensor is a typical application of optical fibers [19,20]. All fiber optical current sensors are typically divided into two categories, where one is based on Faraday effect and the other is based on thermal effect. The former is limited by the extremely small Verdet constant of silica, so in order to increase the device responsivity lots of turns of fibers are needed. A long fiber is necessary to increase the device responsivity because the minimum bend radius of normal optical fiber is a couple of centimeters. The latter needs a short length of fiber but requires complex manufacturing techniques to coat fibers with metals [21–23].

In this paper we demonstrate a compact optical current sensor using an 80mm-long optical fiber micro wire (OFM) with a diameter of 5μm. The OFM was wound for 25 times directly on a 5mm-long, 1mm-diameter copper wire coated with a very thin Teflon film to prevent light coupling. To our knowledge, this is the first time such a miniature optical fiber current sensor is reported.

2. Sensor fabrication and theoretical considerations

Sensor fabrication comprises two-steps. A conventional single mode optical fiber (Corning SMF-28) is tapered into an OFM with a diameter of 5 micrometers using the modified flame-brushing technique [1], with 80mm length of the central uniform taper region. The taper is then wound on a copper wire of length 5mm and diameter 1mm. Two ends of the copper wire are soldered on two pieces of copper plate to facilitate the assembly in an electric circuit with low contact resistance. Before winding, a very thin Teflon layer is coated on the copper wire to prevent leakage losses due to optical coupling from the OFN into the copper wire. The OFM is carefully wound on the copper wire with a large pitch to eliminate optical coupling between adjacent turns. 25 turns were wound on the copper wire with an 80mm-long OFM. The sensor is then packaged with a UV-curable acrylate polymer (Luvantix PC-373). During the fabrication process, the OFM transmission is measured in situ to ensure low insertion loss. Figure 1(a) shows the transmissions of the OFM as a function of wavelength before and after packaging with a total loss of 1.5dB at 1550nm, while Fig. 1(b) shows the packaged sample.

#130605 - $15.00 USD Received 24 Jun 2010; revised 30 Aug 2010; accepted 30 Aug 2010; published 3 Sep 2010

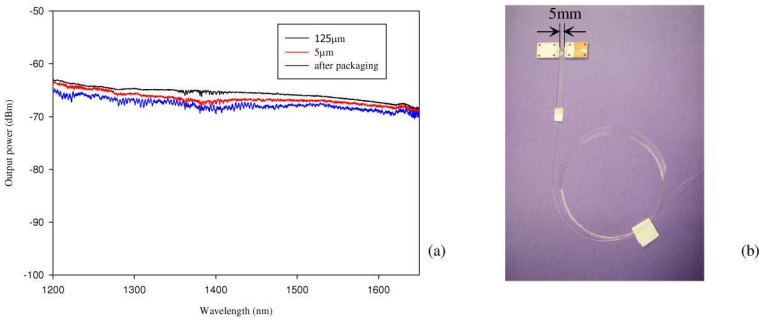

Fig. 1. (a) Experimental results on the fabrication of current sensor. Transmission spectra were recorded before tapering, after tapering and after packaging. (b) Photograph of the packaged OFM coil on the copper wire.

When an alternating current $I_0 \cos(\omega t)$ flows through the copper wire, heat is produced in the wire as:

$$Q_e = I_0^2 R \cos^2(\omega t) = \frac{1}{2} I_0^2 R + \frac{1}{2} I_0^2 R \cos(2\omega t) \tag{1}$$

where R is the resistance of the copper wire, I_0 is the amplitude of current, and ω is the angular frequency of alternating current. The related temperature change of the copper wire is:

$$\Delta T = \frac{Q_e - Q_T}{mC} \tag{2}$$

where Q_T is the heat taken out by thermal conduction, m is the mass of copper wire, C is the specific heat capacity of copper. Because the OFM is in contact with the copper wire, any temperature changes will influence the refractive index and the length of the OFM. The two terms in Eq. (1), show the effect on OFM due to both D.C and A.C components with thermally induced influence from heated copper wire. The DC term can be used as heat phase modulator, but it cannot be easily distinguished from the low frequency drift present in the interferometer system; for this reason here only the AC term is considered. The expression for the phase temperature responsivity of light propagating in a fiber of length L is given by

$$\frac{d\phi}{dT} = \frac{2\pi}{\lambda}\left(n\frac{dL}{dT} + L\frac{dn}{dT} \right) \tag{3}$$

in which n, λ and T are the effective refractive index, wavelength of light and the temperature, respectively. The AC phase can be also be derived as:

$$\phi(t) = \frac{I_0^2 R}{2mC}\frac{2\pi}{\lambda}\left(n\frac{dL}{dT} + L\frac{dn}{dT} \right)\cos(2\omega t) \tag{4}$$

Equation (4) shows that the AC term oscillates at twice the frequency of input current and is proportional to $I_0^2 R$. This change in phase at twice the input current frequency is used to measure the input current.

3. Experiment Results

The experimental layout as shown in Fig. 2, comprises a Michelson interferometer, current transformer and a digital signal processing system. Light from a laser diode (LD) at 1550nm with a linewidth of 0.01nm travels through the optical circulator and is split into two arms of the Michelson interferometer by the 3dB coupler. One arm comprises the current sensor, while the other forms a fiber wrapped round a PZT in order to control the phase by locking at the quadrature point. In order to minimise the polarization dependent noise, both the arms of

#130605 - $15.00 USD Received 24 Jun 2010; revised 30 Aug 2010; accepted 30 Aug 2010; published 3 Sep 2010

the interferometer are terminated in Faraday rotating mirrors (FRM). The interferometer output is sampled by an A/D convertor and recorded by a computer. Due to electromagnetic induction, passage of alternating current through the coil results in a high current being induced in the frame at the same frequency.

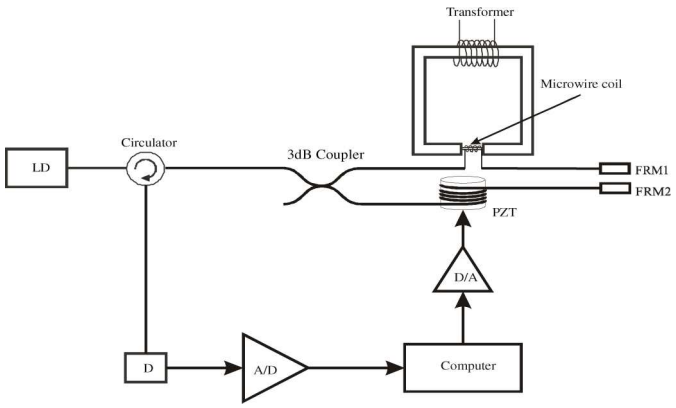

Fig. 2. Diagram of the experimental set-up used to test the sensor. LD stands for laser diode, PZT for piezoelectric transducer, FRM for Faraday rotating mirror, and D for detector.

The current in the frame is measured by a current meter. The interferometer output is sampled by one of A/D convertor channels of National Instrument USB-6221 multifunction data acquisition board. Data is sent to a computer for signal processing. The computer is also used to control the phase bias of the interferometer by adjusting PZT phase modulator through an analog output channel on the USB-6221.

Figure 3 shows the output of the interferometer when a 50Hz, 90A rms alternating current passes through the sensor. Waveform 1 is the detector output, while waveform 2 is the input signal. The frequency of the output signal was measured to be 100Hz, which is in agreement with Eq. (4).

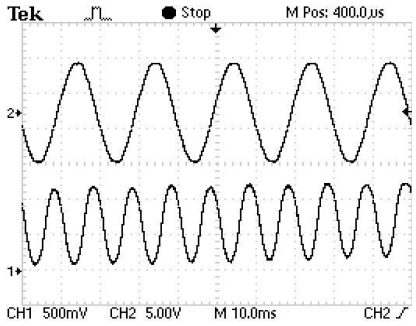

Fig. 3. Output of the current sensor with 90A@50Hz input. The top waveform represents the 50Hz input, while the bottom one is the sensor output.

Responsivity was measured in two different ways. For currents in the range 0 to 40A rms, phase bias control was used. From 45 to 120A rms, harmonics were used to calculate the amplitude of phase modulation [24], and results are shown in Fig. 4. Linear relationship (R^2 = 0.98) between the amplitude of phase modulation and the square of alternating current (1.2A to 120A rms) passing through the copper wire was obtained. Nearly same slopes achieved for the linear fits carried on the data (ref. Fig. 4) corresponding to two different tests suggests repeatability of interferometer phase change measurements with input current. The responsivity of the sensor is 1.28×10^{-4} rad/I^2 at 50Hz. The resistance of the copper wire is

#130605 - $15.00 USD Received 24 Jun 2010; revised 30 Aug 2010; accepted 30 Aug 2010; published 3 Sep 2010

107μΩ. Assuming a minimum-detectable phase change of 10^{-6} rad [25], the observed responsivity at 50Hz corresponds to a minimum detectable current variation of 88mA rms.

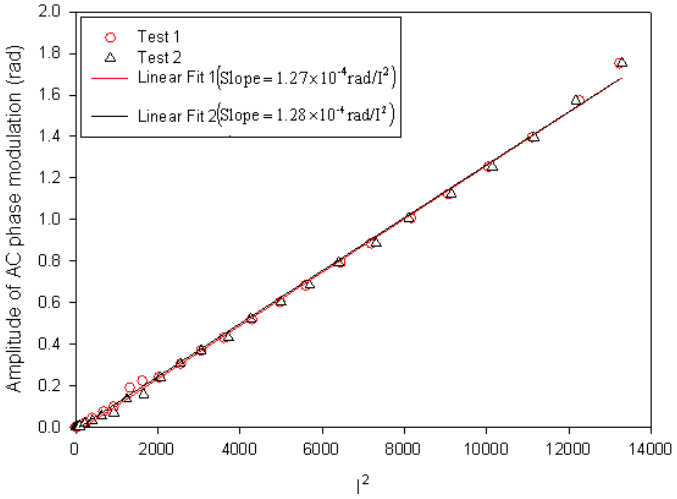

Fig. 4. Amplitude of AC phase measured as a function of square of alternating electric current passing through the copper wire at frequency 50Hz

The sensor response to frequency is presented in Fig. 5. A digital function generator was used to supply currents with different frequencies. The current flowing through the sensor was kept at 9A rms and the current sensor response was recorded. Figure 5 shows that the sensor reponsivity decays for increasing frequencies and is found to be $3.57\times10^{-6}\,\mathrm{rad/I^2}$ at 500Hz.

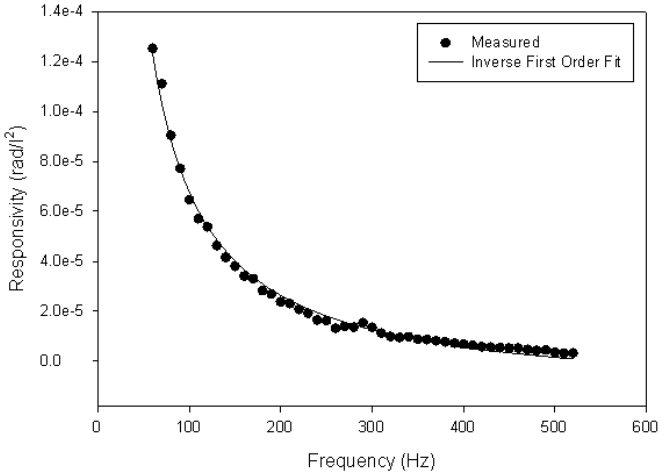

Fig. 5. AC response $\left(\mathrm{rad/I^2}\right)$ of interferometer as a function of driving frequency for heating current sensor

4. Conclusion

In conclusion, we have demonstrated the sensing capabilities of an interferometric current sensor based on optical fiber micro wires. The current sensor comprised an optical fiber micro wire wrapped round a 1mm-diameter copper wire over a length of 5mm. Success with such compact designs opens possibilities for even smaller copper support rods, carrying current. The sensor was tested in an optical fiber Michelson interferometer configuration with a phase

#130605 - $15.00 USD Received 24 Jun 2010; revised 30 Aug 2010; accepted 30 Aug 2010; published 3 Sep 2010

responsivity of 1.28×10^{-4} rad/I^2 at 50Hz with an input impedance of 107μΩ. However, the responsivity was found to vary inversely with increasing frequencies, and was shown to be 3.57×10^{-6} rad/I^2 for a frequency of 500Hz. Responsivity can be increased by reducing the diameter of the copper wire or increasing the material electrical resistivity.

Acknowledgments

GB gratefully acknowledges the Royal Society (London, U.K.) for his research fellowship. The authors thank the Engineering and Physical Sciences Research Council (EPSRC) for financial support. Z. Song is grateful to CSC for his academic visitor scholarship.

#130605 - $15.00 USD Received 24 Jun 2010; revised 30 Aug 2010; accepted 30 Aug 2010; published 3 Sep 2010